# A New Robust Interference Reduction Scheme for Low Complexity Direct-Sequence Spread-Spectrum Receivers: Performance

Alois M.J. Goiser, Samar Khattab, Gerhard Fassl
*Institute of Communications and Radio Engineering*
*University of Technology Vienna*
*Vienna, Austria*
*Email: alois.goiser@tuwien.ac.at*

Ulrich Schmid
*Department of Computer Engineering*
*University of Technology Vienna*
*Vienna, Austria*
*Email: s@ecs.tuwien.ac.at*

***Abstract*—In this paper, we present a new robust direct-sequence spread-spectrum concept with integrated interference reduction capabilities to reduce mixed narrowband- and broadband-interference. It combines robustness in the presence of strong interference of unknown composition with implementation simplicity and spectral efficiency. This is achieved by combining a comparatively low processing gain direct-sequence spread-spectrum system with an efficient interference reduction technique based on a simple adaptive nonlinearity employed prior to spread-spectrum demodulation. Our reliable chip accumulation technique allows to combine spectral efficiency with interference reduction capabilities comparable to traditional military spread-spectrum systems, which typically rely on a huge processing gain that is not affordable in commercial bandwidth-limited applications.**

***Keywords*-Interference Reduction, Reliable Communication, Robust Communication, Spread-Spectrum, Nonlinear Signal Processing, Continuous-Wave Interference.**

## I. Introduction

During recent years, both the number of deployments and the properties/requirements of applications of wireless networks have tremendously evolved. The spectrum ranges from cellular networks, which employ a fixed infrastructure of base stations supporting a large number of mobile devices, to wireless sensor networks, where a huge number of small devices create their own communications infrastructure. Increasingly, wireless networks are also being considered as an alterative to wired networks in critical application domains like aerospace and automotive [1]: Given that high-end cars are equipped with something like 50+ embedded microcontrollers nowadays, replacing the classic wireline interconnect by a wireless network is indeed attractive in terms of costs and flexibility.

Such applications pose new challenges to wireless communication technology, however: Enabling reliable real-time communication between low-cost network nodes with limited resources and power consumption, in the presence of harsh, typically unknown and varying environmental conditions. Obviously, such a setting does not match well the assumptions underlying most state-of-the-art wireless solutions, which employ complex receivers designed for optimal performance under certain channel conditions. We argue that there is a need for *robust* wireless communication approaches, which perform acceptable under a wide variety of channel conditions, and admit a simple and efficient implementation.

In this paper, we present concept and theoretical performance analysis of such a robust wireless communication approach, termed *reliable chip accumulation* (RCA) detector: It combines an efficient new interference reduction technique based on a simple nonlinearity with a conventional direct-sequence spread-spectrum system with comparatively low process gain, which is mandatory for achieving a spectral efficiency that is suitable for commercial applications.

Originally, the spread-spectrum concept was invented for military applications. Military interests like low probability of intercept and covered communication are strictly related to a large processing gain, which in turn result in a large bandwidth of the spread-spectrum signal (channel signal). Since the potential interference reduction capability of a spread-spectrum system is also directly related to the processing gain, military solutions inherently provide a suitably low symbol-error probability also in the presence of interference. The bandwidth limitations for commercial applications do not allow comparable processing gains, which calls for alternative interference reduction techniques to improve the signal-to-noise ratio. Our RCA detector employs a simple adaptive nonlinearity for this purpose.

We evaluate the performance of our solution in the presence of strong permanent interference combined from two unwanted signal sources with extreme frequency distributions: A broadband source modeled as additive-white gaussian-noise (AWGN) interference, and a narrowband source modeled as continuous-wave (CW) interference. The ratio of AWGN- and CW-interference is allowed to change in a wide range (more than 40 dB). Theoretical and our simulation results will show that our RCA detector has an excellent performance in all these settings. In this paper, we focus on the case where the threshold used for adapting the nonlinearity is chosen optimally. In a companion paper [9], we describe an implementation of a suitable threshold

adaption technique and the resulting performance of the RCA detector when using this scheme.

After an overview of our solution and related work in Section II, we start with the detailed description of the interference environment in Section III. The detailed structure of the RCA detector is outlined in Section IV, where the interference reduction mechanism of the proposed nonlinearity is emphasized. The theoretical performance of the pre-detection nonlinear signal processing is treated in Section V. The theoretical performance of the proposed detector is evaluated in Section VI by means of the symbol-error-probability (SEP).

## II. Overview and related work

In Fig. 1, the structure of the proposed interference reduction scheme is shown. It involves a two step process: The first step exploits the interference reduction capability of the well known plain spread-spectrum technology with its unique processing gain [2]. The reasons why we use the spread-spectrum technology as basic modulation scheme is summarized in [8]. In addition, prior to the spread-spectrum demodulation, a second interference reduction scheme refered to as the reliable chip accumulator (RCA) is used. The nonlinear processing involved in RCA is done by a simple and memoryless nonlinearity the reliable chip selector RCS. Splitting the involved mechanisms allows us to take advantage of two different means for interference reduction: Spread-spectrum technology exploits bandwidth expansion for this purpose, whereas RCS exploits a nonlinear input/output relation to reduce the magnitude of the interference without bandwidth expansion.

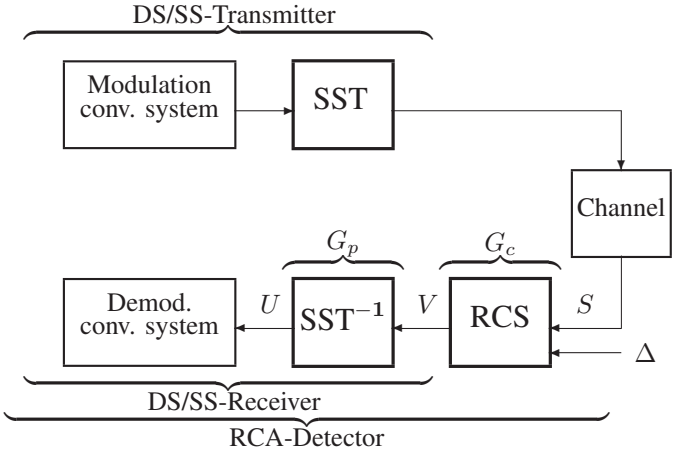


Figure 1. Structure of the investigated communication system. SST ... spread-spectrum technology, DS/SS ... direct-sequence spread-spectrum, RCS ... reliable chip selector, RCA ... reliable chip accumulator, $G_p$ ... processing gain, $G_c$ ... conversion gain, $\Delta$ ... threshold, $S, V, U$ ... random variables.

The potential capability for system performance improvement using interference reduction schemes is manifested in the literature by many authors. We pick only two as representatives [3], [4].

To achieve a high degree of flexibility we choose a digital receiver architecture to gain the following advantages: (a) Simple and cheap signal processing, (b) limited word-length for information mapping, (c) easy to store, easy channel-coding and encryption. Much of the complexity of a digital receiver is determined by the word-length of the necessary analog-to-digital conversion prior to the correlation. One-bit quantization (hard-limiter) has the lowest implementation complexity, but provides the most coarse quantization: For AWGN-interference, the resulting reduction in the signal-to-noise ratio (SNR) prior to detection is about 2 dB, which can be accepted. For narrowband interference, however, the degradation of the SNR can be more than 7 dB, which is not acceptable [5], [6]. Multibit quantization would raise the receiver complexity, which is not our goal: For cost reasons, the core of the spread-spectrum symbol detection in our receiver shall be a single bit digital correlator.

Our solution to this problem is a sophisticated quantization procedure; from a complexity point of view, we process only one-bit quantized signals in the symbol detection procedure. But the one-bit quantized signal is constructed from a simple but adaptive nonlinearity, which allows to avoid the loss of information in the signal of interest commonly caused by coarse quantization: Our RCA scheme reduces mainly the information of the signals of no interest, which offers the potential capability to improve the SNR prior to detection. We will demonstrate that it is indeed possible to trade-in complexity for some sophisticated but simple adaptive nonlinear signal processing, without losing a performance comparable to complex solutions and significant improvements over non-adaptive systems. The resulting transceiver combines the advantages of low complexity digital signal processing with the advantage of interference reduction in a single step.

## III. Interference environment

The bottom layer of the interference environment is permanent and constant AWGN. Additional to the broadband AWGN ($n(t)$), a strong continuous-wave interference ($i(t)$) is present to represent the narrowband interference. The involved signals are given in (1). A pictorial view of the received and to baseband converted signal is sketched in Fig. 2. The transmitter and channel model are presented in Fig. 3.

$$\begin{aligned} s(t) &= A_{cw}\,\sin(2\pi f_{cw} t + \varphi) + n(t) + A_c\, D_n\, p(t)\, c(t) = \\ &= i(t) + n(t) + g(t) \end{aligned} \tag{1}$$

In dealing with interference reduction, it is useful to identify the involved signals with its relevance for the detection process. Therefore we refer to the signal we want to detect as signals of interest (SOI). This indicates that

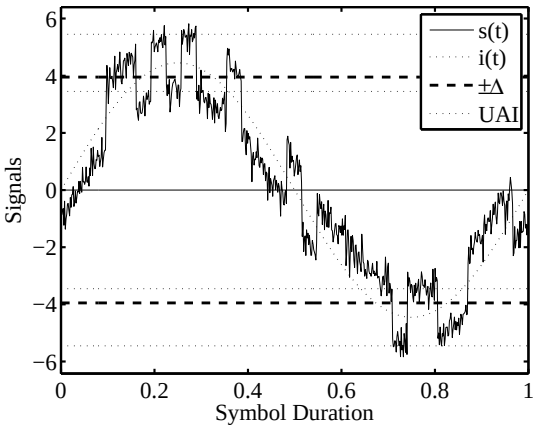


Figure 2. Sample of the investigated input signal (unfiltered). UAI ... unambiguous interval.

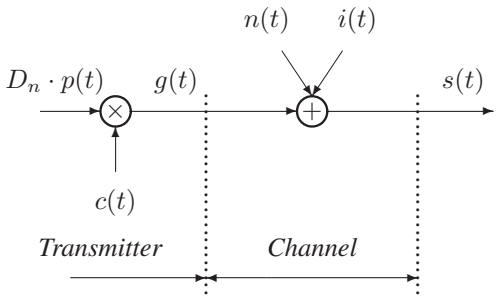


Figure 3. Transmitter and channel model. $p(t)$ ... unite rectangular pulse, $D_n$ ... n-th databit, $c(t)$ ... spread-spectrum signal, $g(t)$ ... SOI, $n(t), i(t)$ ... SONI, $s(t)$ ... received signal.

the information carried by that signal is a valuable one. All other signals that carry no user information are termed signals of no interest (SONI). In our case (compare (1) and Fig. 3) the signal $g(t)$ is the SOI and the signals $i(t)$ and $n(t)$ are the SONI. The signal $c(t)$ is the direct-sequence spread-spectrum signal, $p(t)$ is the unit pulse function, $D_n \in \{\pm 1\}$ indicates the actual data-bit and $A_{cw}$ and $A_c$ are the continuous-wave magnitude and the magnitude of the spread-spectrum signal, respectively. We define in (2) a general signal-to-total-interference ratio (SINR). In (2) the $\text{SINR}_s$ at the input of the adaptive nonlinearity is shown. For the combined interference some characteristic magnitude ranges appear. The unambiguous interval (UAI) is the range at the top of the CW-magnitude with $\pm A_c$ ranging from the inner boundary (IB) located at $A_{cw} - A_c$ to the outer boundary (OB) located at $A_{cw} + A_c$

$$\text{SINR}_s = \frac{2A_c^2}{A_{cw}^2 + 2\sigma_n^2} \tag{2}$$

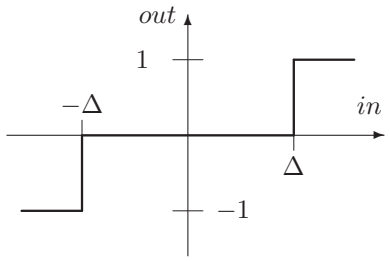


Figure 4. Transfer characteristic of the reliable chip selector (RCS).

## IV. Adaptive Interference Reduction

In this section, we explain the interaction and the overall behavior of the two independent interference reduction schemes. The spread-spectrum concept offers the processing gain $G_p$ to combat the interference. Before the signal is presented to the spread-spectrum demodulation it is processed in an additional interference reduction block. In that block the received signal is processed by an adaptive nonlinearity. The interference reduction capability of the spread-spectrum technology is assumed to be known and discussed in [2]. Here, we emphasize the interoperability of both interference reduction schemes.

In conventional digital communication systems, the symbol-error-probability is directly related to the SNR at the input to the decision stage (hard decision). Maximizing the SNR means to maximize the reliability of the decision. In the conventional correlation detector the whole signal is processed in one shot. In our system we divide the symbol-decision in sub-decisions to maximize the amount of reliable decisions. This allows us to limit the effect of the interference in the sub-decisions.

The spread-spectrum technology offers with the direct-sequence signal a very natural way to partition the symbol-decision into a number of chip-decisions. A different point of view to the partitioning into chip-decisions is the avoidance of the so called "capture-effect". The nature of the capture effect is that the wanted signal is shifted in magnitude to an extent where the usual binary decision based on the polarity of the SOI is meaningless. The RCA scheme avoids this situation and gives the sub-decisions (chip-decisions) its original meaning back.

The form of the adaptive nonlinearity is derived from two assumptions: (a) Unreliable signal magnitudes are erased and not included in the symbol decision process, and (b) the reliable magnitudes are included in the decision process only with their polarity (coarsest magnitude resolution). That means that the received signal has to pass an erasure zone or to undergo a quantization operation. This course signal processing is implemented with the nonlinearity shown in Fig. 4. Due to that simple operations we need at least one

degree of freedom to react to changes of the combined interference. This freedom is achieved with the threshold $\Delta$. The variation of $\Delta$ defines the erasure zone in the magnitude space of the received signal. The adaptation of $\Delta$ is done in accordance with the composition of the interference. This is the subject in [9].

## V. Theoretical Performance of the Adaptive Nonlinearity

From Fig. 1 we derive that the final symbol decision is done by correlation detection and hard decision in the spread-spectrum demodulator. Therefore the symbol-error-probability is directly related to the SINR at the correlator input and the unique processing gain $G_p$ of the spread-spectrum technology. The SINR at the correlator input equals the $\text{SINR}_v$ from the RCS output. What we know and have available is the $\text{SINR}_s$ at the RCS input. From that point of view it is straight forward to define a conversion gain which relates the $\text{SINR}_s$ at the input to the $\text{SINR}_v$ at the output.

$$G_c = \frac{\text{SINR}_v}{\text{SINR}_s} \qquad \text{.... Conversion Gain} \tag{3}$$

The performance evaluation is based on SINR that indicates that a second order statistic was chosen. In the next section we calculate the conversion gain by evaluating the output $\text{SINR}_v$. Then we calculate the symbol-error-probability with (4).

$$\text{SEP} = \frac{1}{2} \cdot \mathit{erfc}\left(\sqrt{\frac{G_c\, G_p}{2} \cdot \text{SINR}_s}\right) \tag{4}$$

From (4) it is obvious that the conversion gain makes the difference to the plain spread-spectrum system and it offers the possibility to trade-off processing gain with conversion gain. Therefore the rest of the paper deals with the evaluation of the conversion gain and the achievable symbol-error-probability.

### A. Mathematical Calculation of the Conversion Gain

In this section we develop the theoretical conversion gain for the reliable chip accumulator. First we calculate the probability density of the input signal (5). The output probability density is a delta distribution (6) and the derived $\text{SINR}_v$ is given in (7). The dependency on the output delta distribution from the threshold $\Delta$ is defined in (8).

One remark before we present a more detailed view of the derivative for the conversion gain. For data-detection we route only the reliable chip magnitudes to the correlation process. Therefore in the calculation for the output $\text{SINR}_v$ the probabilities $P_1$ and $P_{-1}$ occur. The also available probability $P_0$ is a useful measure for the ratio of rejected chips (CRR) and is defined in (9).

The probability density function for the SONI at the input is derived from the random variable $Z = X + Y$ which is

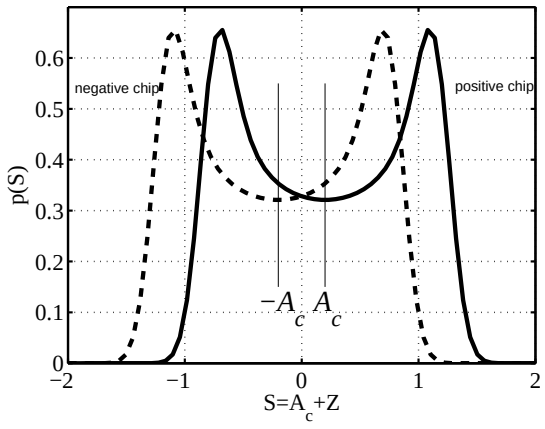


Figure 5. Normalized probability density at the input of the RCS for a positive chip. I/N=-15 dB and SINR=-40 dB.

the addition of two independent random variables $X$ representing the continuous-wave interference and the random variable $Y$ which represents the AWGN interference. Both can be assumed to be independent. If a positive chip from the SOI (with magnitude $A_c$) is presented to the input, the probability density $p_z(Z)$ of the SONI is shifted to the right by $A_c$. The new random variable at the input is $S = A_c + Z$. Verify Fig. 5. For further details in the derivative of the input probability density we refer to [7]. Due to the balanced nature of the direct-sequence signal and assuming a fair binary source it is only necessary to investigate a positive chip to calculate the $\text{SINR}_v$ at the output of the RCS.

$$\begin{aligned} p_z(Z) &= p_x(Z) * p_y(Z) = \int_{-\infty}^{+\infty} p_x(X) p_y(Z-X)\, dX \\ &= \frac{1}{\pi\sqrt{2\pi}\sigma_n} \int_{\varphi=-\frac{\pi}{2}}^{\varphi=\frac{\pi}{2}} e^{-\frac{1}{2\sigma_n^2}(Z - A_{cw}\cdot\sin\varphi)^2} d\varphi \qquad (5) \\ &= \frac{1}{\sqrt{2\,\pi}\,\sigma_n} \sum_{n=0}^{\infty} \frac{\left(-\frac{Z^2}{2\,\sigma_n^2}\right)^n}{n!} \cdot {}_1F_1\Big[n + \frac{1}{2}\,;\, 1\,;\, -\frac{A_{cw}^2}{2\,\sigma_n^2}\Big] \end{aligned}$$

$$\begin{aligned} \text{E}[\,V\,] &= P_1 - P_{-1} \\ \text{E}[\,V^2\,] &= P_1 + P_{-1} \end{aligned} \tag{6}$$

$$\text{SINR}_v = \frac{\text{E}^2[\,V\,]}{\text{Var}[\,V\,]} = \frac{\text{E}^2[\,V\,]}{\text{E}[\,V^2\,] - \text{E}^2[\,V\,]} \tag{7}$$

$$\begin{aligned} P_1(\Delta) &= \Pr[\,V=1\,] = \Pr[\,S = Z + A_c > \Delta\,] \\ &= \Pr[\,Z > \Delta - A_c\,] = 1 - \Pr[\,Z \le \Delta - A_c\,] \\ P_{-1}(\Delta) &= \Pr[\,V=-1\,] = \Pr[\,S = Z + A_c \le -\Delta\,] \\ &= \Pr[\,Z \le -\Delta - A_c\,] \qquad (8) \\ P_0(\Delta) &= \Pr[\,V=0\,] = \Pr[\,-\Delta < S = Z + A_c \le \Delta\,] \\ &= 1 - P_1 - P_{-1} \end{aligned}$$

$$\text{CRR} = P_0 \qquad \text{.... Chip Rejection Ratio} \tag{9}$$

The RCS maps a certain magnitude range from its input to a certain level ($\pm 1$). For this mapping the integral in (10) is useful and applied in (11). With (11) we are able to formulate the $\text{SINR}_v$ in (12) and finally the conversion gain in (13).

$$\Pr\left[\, Z < \Delta \mid \Delta > 0 \,\right] = \frac{1}{2} + \underbrace{\int_{z=0}^{\Delta} p_z(Z)dZ}_{I} \tag{10}$$

$$I = \frac{1}{\sqrt{2\pi}\sigma_n} \sum_{n=0}^{\infty} \frac{\left(-\frac{1}{2\sigma_n^2}\right)^n}{n!} \cdot {}_1F_1\Big[n+\frac{1}{2};1;-\frac{A_{cw}^2}{2\sigma_n^2}\Big] \cdot \int_{z=0}^{\Delta} Z^{2n} dZ$$

$$= \underbrace{\frac{1}{\sqrt{2\,\pi}\sigma_n}}_{a} \sum_{n=0}^{\infty} \underbrace{\frac{\left(-\frac{1}{2\sigma_n^2}\right)^n}{n!(2n+1)}}_{b_n} \cdot \underbrace{{}_1F_1\Big[n+\frac{1}{2};1;-\frac{A_{cw}^2}{2\sigma_n^2}\Big]}_{F_{11,n}} \cdot \Delta^{2n+1}$$

$$\begin{aligned} P_1(\Delta) &= \Pr\left[\, s(t) > \Delta \,\right] \\ &= \frac{1}{2} - a \cdot \sum_{n=0}^{\infty} b_n \cdot F_{11,n} \cdot (\Delta - A_c)^{2n+1} \\ P_{-1}(\Delta) &= \Pr\left[\, s(t) \le -\Delta \,\right] = \\ &= \frac{1}{2} - a \cdot \sum_{n=0}^{\infty} b_n \cdot F_{11,n} \cdot (\Delta + A_c)^{2n+1} \end{aligned} \tag{11}$$

$$\text{SINR}_v(\Delta) = \frac{(P_1 - P_{-1})^2}{P_1 + P_{-1} - (P_1 - P_{-1})^2} = \left[\frac{T_1}{T_2^2} - 1\right]^{-1} \tag{12}$$

$$\begin{aligned} T_1 &= P_1 + P_{-1} = \\ &= 1 - \frac{1}{\sqrt{2\pi}\sigma_n} \sum_{n=0}^{\infty} \frac{\left(\frac{-1}{2\sigma_n^2}\right)^n}{n!(2n+1)} \cdot {}_1F_1\Big[n+\frac{1}{2};1;-\frac{A_{cw}^2}{2\sigma_n^2}\Big] \cdot \\ &\quad \cdot \Big\{ (\Delta + A_c)^{2n+1} + (\Delta - A_c)^{2n+1} \Big\} \\ T_2 &= P_1 - P_{-1} = \\ &= \frac{1}{\sqrt{2\pi}\sigma_n} \sum_{n=0}^{\infty} \frac{\left(\frac{-1}{2\sigma_n^2}\right)^n}{n!(2n+1)} \cdot {}_1F_1\Big[n+\frac{1}{2};1;-\frac{A_{cw}^2}{2\sigma_n^2}\Big] \cdot \\ &\quad \cdot \Big\{ (\Delta + A_c)^{2n+1} - (\Delta - A_c)^{2n+1} \Big\} \end{aligned}$$

$$G_c(\Delta) = \frac{\text{SINR}_v(\Delta)}{\text{SINR}_s} = \left[\frac{T_1}{T_2^2} - 1\right]^{-1} \cdot \left[\frac{2A_c^2}{A_{cw}^2 + 2\sigma_n^2}\right]^{-1} \tag{13}$$

To verify our calculation for the conversion gain we use the well known and most frequently encountered result available in the literature the conversion gain for the hard limiter stimulated with AWGN. Therefore we specify (12) by setting $A_{cw} = 0$ and $\Delta = 0$ and achieve (14). In the series development we neglect all terms accept the first. Additionally we use the low SNR assumption which is a perfect match to spread-spectrum communication. The result (15) is in agreement with the results derived in [5], [6].

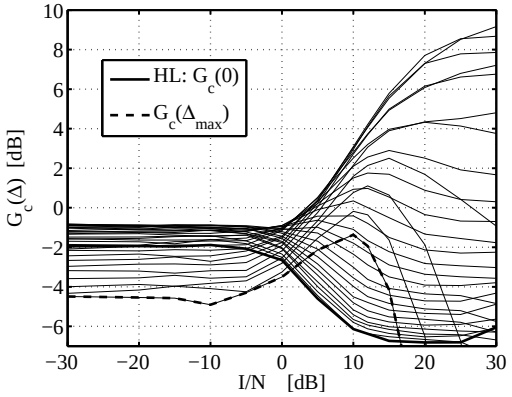


Figure 6. Theoretical conversion gain of the RCS for a positive chip $A_c$=1 V. The threshold $\Delta$ varies from 0 Volt to 10 Volt. $\text{SINR}_s$=-15 dB.

$$\textit{SNR}_v(0) = \left[\left(\sqrt{\frac{2}{\pi} \cdot \textit{SNR}_s} \sum_{n=0}^{\infty} \frac{\left(\frac{-1}{2}\right)^n}{n!(2n+1)} (\textit{SNR}_s)^n\right)^{-2} - 1\right]^{-1} \tag{14}$$

$$G_c(0) = \frac{\textit{SNR}_v(0)}{\textit{SNR}_s} = \frac{2}{\pi}\Big[1 - \frac{2}{\pi} \cdot \underbrace{\textit{SNR}_s}_{\to 0}\Big]^{-1} = \frac{2}{\pi} \mapsto -1.96\ dB \tag{15}$$

### *B. Discussion of the Conversion Gain*

Now we discuss the results for the conversion gain. We start with a field of theoretical conversion gains $G_c(\Delta)$ from (13) plotted in Fig. 6. For better verification we investigate different interference scenarios ranging form dominating AWGN-interference to dominating continuous-wave interference. The input $\text{SINR}_s$=-15 dB. The field parameter is the threshold $\Delta$. The hard-limiter, as one extreme in the derivative, behaves as the theory states. In dominating AWGN-interference we verify the value (15) of -1.96 dB and for dominating CW-interference about -7 dB [5].

The general tendency of the conversion gain for well adjusted thresholds is the following: (a) in dominating AWGN-interference we achieve a conversion gain of about one Decibel compared to the hard-limiter, (b) in dominating CW-interference the RCS show superior performance against the hard-limiter with roughly 15 dB.

The primary results for engineers are presented in Fig. 7. Because in this figure we have extracted the optimum curve $G_c(\Delta_{opt})$ from the field in Fig. 6. For each ratio of I/N we have selected the maximum of the conversion gain ($\max\left(G_c(\Delta)\right) = G_c(\Delta_{opt})$) and the related threshold $\Delta_{opt}$.

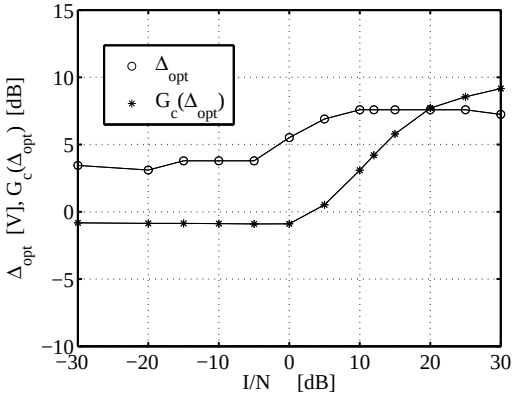


Figure 7. Theoretical optimum conversion gain and optimum threshold for the RCS for a positive chip $A_c$=1 V. SINR$_s$=-15 dB.

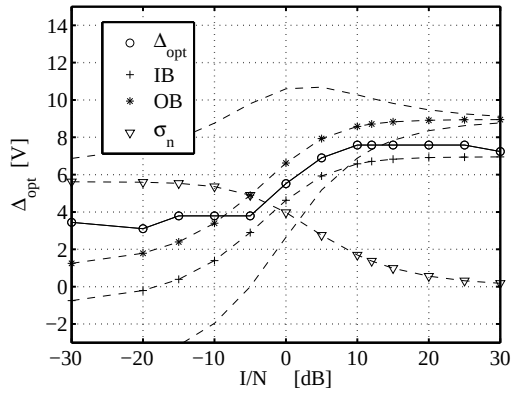


Figure 8. Theoretical optimum threshold for the RCS with other relevant signal parameters for a positive chip $A_c$=1 V. SINR$_s$=-15 dB. Dashed line: $A_{cw} + A_c \pm \sigma_n$

It is an engineering task to find a way to adjust the threshold on its optimum location and track this optimum location in a changing interference environment [9].

To make the result more transparent we sketch in Fig. 8 the optimum threshold with relevant signal parameters. For dominant CW the location of the optimum threshold $\Delta_{opt}$ is within the UAI and close to the IB which indicates that for this location the maximum number of reliable chip decisions occur. If the interference changes to dominating AWGN-interference the optimum location for the threshold is outside the UAI. This can be verified when the standard deviation of the AWGN interference is encountered (dashed line in Fig. 8).

From Fig. 9 to Fig. 12 we sketch sample-functions of the input and output signals of the HL and the RCS for a positive chip ($A_c = 1$ V) with their corresponding probabilities $P_1, P_{-1}, P_0$. For the RCS a threshold close to the optimum threshold is chosen. The results are derived with simulations to verify the theoretical conversion gain in Fig. 6.

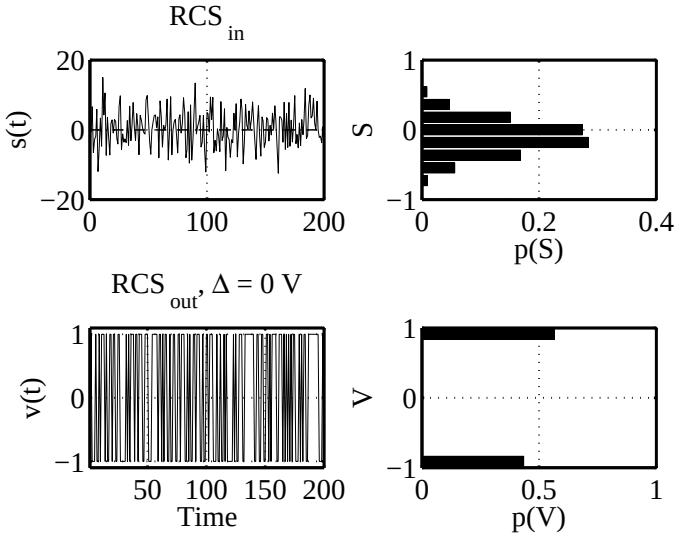


Figure 9. Sample-function of the HL input and output for a positive chip $A_c$=1 V. CRR=0%, $G_c$=-2.0 dB. Parameters: I/N=-30 dB, $\Delta$=0 V, SINR$_s$=-15 dB.

The HL transfer all input magnitudes, quantized to $\pm 1$, to the output (CRR=0%). The conversion gain in dominating AWGN (Fig. 9) is -2 dB and agrees with (15) and Fig. 6. The conversion gain in dominating CW-interference (Fig. 11) is down to a value of about -6 dB and in agreement with Fig. 6 and [5].

The RCS erase magnitudes from the input signal. For dominating AWGN-interference (Fig. 10) the CRR is about 50% and the conversion gain is about -0.8 dB which is about 1.2 dB better than the HL. In dominating CW-interference (Fig. 12) the CRR is about 80% and the conversion gain is about 8.8 dB which is about 16 dB better than the HL.

## VI. Symbol-Error-Probability

The symbol-error-probability (4) is sketched in Fig. 13. The conclusion derived from the SEP is that the performance of the HL-detector is rather bad in CW dominated interference. The strong CW magnitude completely captures the weak direct-sequence signal (SOI). Only the proposed RCA-detector can handle the capture effect due to its threshold concept and show superior performance in CW dominated environments. In AWGN dominated interference the RCA always outperforms the HL-detector. This offers the possibility to trade-off processing gain (bandwidth expansion) with nonlinear signal processing.

## References

[1] T. Nolte, H. Hansson, and L. L. Bello: *Wireless Automotive Networks*. Proceedings RTN'05, 35-38, 2005.

[2] M.K. Simon, J.K. Omura, R.A. Scholtz, and B.K. Levitt, *Spread Spectrum Communications Handbook*, McGraw-Hill, Inc., ISBN 0-07057629-7, 1994.

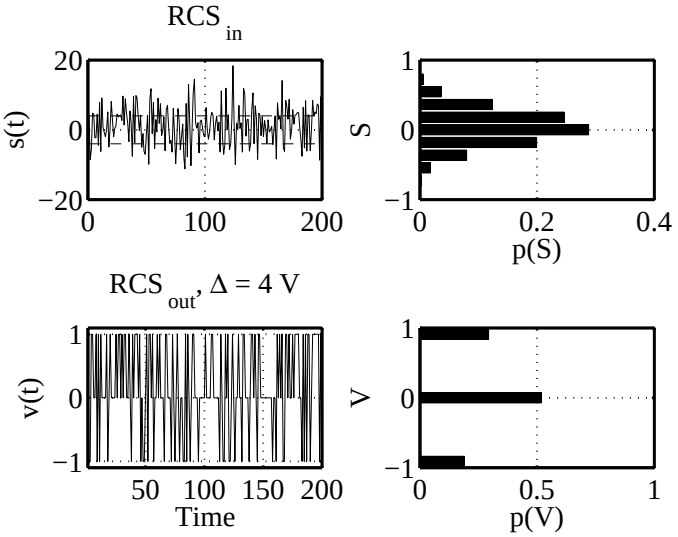


Figure 10. Sample-function of the RCS input and output for a positive chip $A_c$=1 V. CRR=50%, $G_c$=-0.8 dB. Parameters: I/N=-30 dB, $\Delta$=4 V, SINR$_s$=-15 dB.

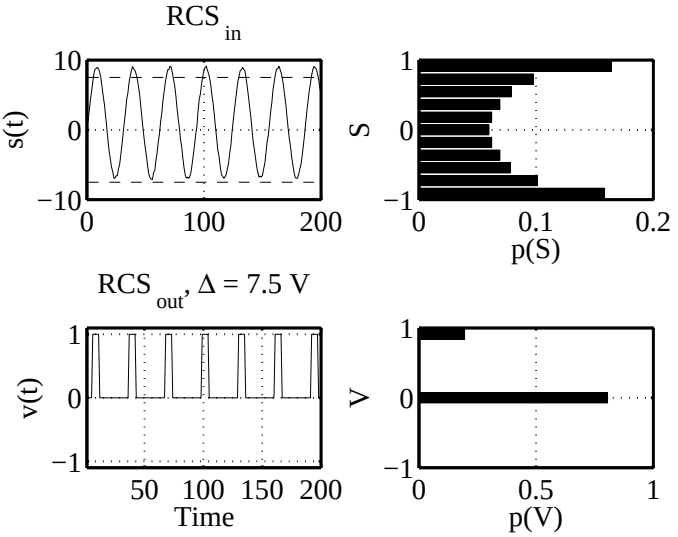


Figure 12. Sample-function of the RCS input and output for a positive chip $A_c$=1 V. CRR=80%, $G_c$=8.8 dB. Parameters: I/N=30 dB, $\Delta$=7.5 V, SINR$_s$=-15 dB.

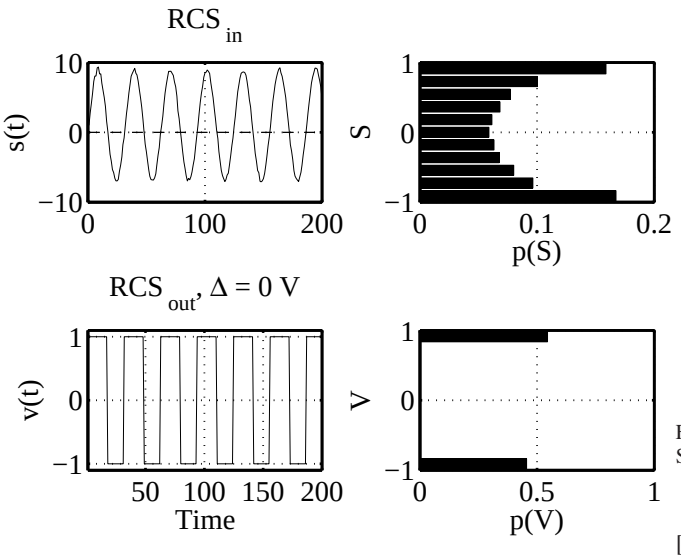


Figure 11. Sample-function of the HL input and output for a positive chip $A_c$=1 V. CRR=0%, $G_c$=-6.0 dB. Parameters: I/N=30 dB, $\Delta$=0 V, SINR$_s$=-15 dB.

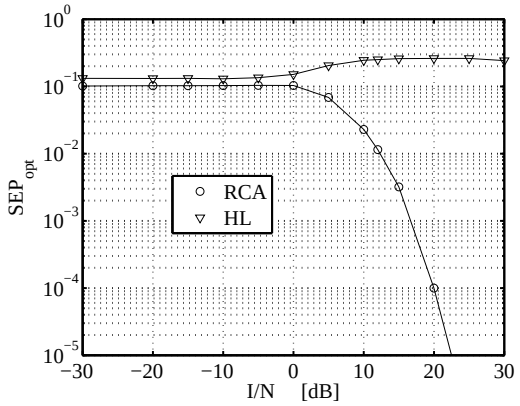


Figure 13. Theoretical symbol-error-probability for $G_p$=15 dB and SINR$_s$=-15 dB.


[3] L.B. Milstein, *Interference Rejection Techniques in Spread-Spectrum Communications*, IEEE Proceedings, Vol. 76, No. 6, 1988.

[4] J.D. Laster, and J.H. Reed, *Interference Rejection in Digital Wireless Communications*, IEEE Signal Processing Magazin, 37-62, 1997.

[5] W.Davenport Jr., *Signal-to-Noise Ratios in Band-Pass-Limiters*, Journal of Applied Physics, Vol. 24, Nr. 6, 720-727, 1953.

[6] James J. Spilker, Jr., *Digital Communications by Satellite*, Prentice-Hall, 1977.

[7] A. Goiser, *Enhancing the Signal-to-Interference Ratio in Digital Direct-Sequence Spread-Spectrum Receivers*, International Journal of Wireless Information Networks, Plenum-Press, August, 173-186, 1997.

[8] A. Goiser, and S. Khattab, *Robust and Reliable Communication Meets Future Mobile Communication Demands*, Proceedings ICAS2010, 176-181, 2010.

[9] A. Goiser, S. Khattab, G. Fassl, and U. Schmid *A New Robust Interference Reduction Scheme for Low Complexity Direct-Sequence Spread-Spectrum Receivers: Optimization*, in press, Proceedings NexComm2010, 2010.